World J Microbiol Biotechnol (2017) 33:86
DOI 10.1007/s11274-017-2255-0

ORIGINAL PAPER

# Comparative metagenomics reveals insights into the deep-sea adaptation mechanism of the microorganisms in Iheya hydrothermal fields

**Hai-liang Wang**[1,2,3] · **Li Sun**[1,2]

Received: 7 June 2016 / Accepted: 31 March 2017 / Published online: 6 April 2017


**Abstract** In this study, comparative metagenomic analysis was performed to investigate the genetic profiles of the microbial communities inhabiting the sediments surrounding Iheya North and Iheya Ridge hydrothermal fields. Four samples were used, which differed in their distances from hydrothermal vents. The results showed that genes involved in cell surface structure synthesis, polyamine metabolism and homeostasis, osmoadaptation, pH and $Na^+$ homeostasis, and heavy-metal transport were abundant. Pathways for putrescine and spermidine synthesis and transport were identified in the four metagenomes, which possibly participate in the regulation of cytoplasmic pH. Genes involved in the transport of $K^+$ and the biosynthesis of glycine betaine, proline, and trehalose, together with genes encoding mechanosensitive channel of small conductance, were contributors of osmoadaptation. Detection of genes encoding $F_1F_o$-ATPase and cation/proton antiporters indicated critical roles played by pH and sodium homeostasis. $Cu^{2+}$-exporting and $Cd^{2+}/Zn^{2+}$-exporting ATPases functioned in the expulsion of toxic metals across cellular membranes. It is noteworthy that the distribution of some genes, such as that encoding cardiolipin synthase, was apparently affected by distance to the vent site. These findings provide insight into microbial adaptation mechanisms in deep-sea sediment environments.

**Keywords** Hydrothermal vent · Sediment · Metagenomics · Environmental adaptation

## Introduction

Deep-sea environments, including hydrothermal vents, are the most extended extreme environments on Earth, and are characterized by high hydrostatic pressures and absence of light (Prieur et al. 1995). In hydrothermal vents, in addition to extreme physical parameters, there exist extremely steep chemical, pH, and temperature gradients between vent fluids and the surrounding seawater (Thornburg et al. 2010).

Okinawa Trough is an active back-arc basin located behind the Ryukyu trench and Ryukyu Islands (Glasby and Notsu 2003). A number of hydrothermal fields have been found in this area, including those in Iheya North and Iheya Ridge fields (Glasby and Notsu 2003; Tokeshi 2011). The community structures of macrobenthic and microbial communities in different hydrothermal fields have been investigated by several research groups (Ohta and Kim 2001; Tokeshi 2011; Yanagawa et al. 2013; Zhang et al. 2015). It was reported that microbial communities inhabiting the sediments of Iheya North and Iheya Ridge hydrothermal fields have a higher bacterial diversity and a lower archaeal diversity, and that Proteobacteria and Thaumarchaeota are the dominant bacterial and archaeal populations, respectively (Wang and Sun 2016; Zhang et al. 2015).

Mid-Okinawa Trough is covered with terrigenous thick organic matter-enriched sediments mainly derived from

**Electronic supplementary material** The online version of this article (doi:10.1007/s11274-017-2255-0) contains supplementary material, which is available to authorized users.

✉ Li Sun
lsun@qdio.ac.cn

[1] Key Laboratory of Experimental Marine Biology, Institute of Oceanology, Chinese Academy of Sciences, 7 Nanhai Road, Qingdao 266071, China

[2] Laboratory for Marine Biology and Biotechnology, Qingdao National Laboratory for Marine Science and Technology, Qingdao, China

[3] University of Chinese Academy of Sciences, Beijing, China

the Yangtze and Yellow Rivers (Katayama and Watanabe 2003; Sibuet et al. 1987). The chemistry of the submarine hydrothermal fluids in the vicinity of mid-Okinawa Trough is unusual compared to other deep-sea hydrothermal fluids (Tsuji et al. 2012). In Iheya Ridge, hydrothermal fluids discharged from vent orifices usually have a high concentration of ammonia and a high alkalinity due to fluid-sediment interactions (Gamo et al. 1991; Sakai et al. 1990). By contrast, hydrothermal fluids discharged from Iheya North Knoll have a lower ammonia concentration and alkalinity indicating less extensive fluid-sediment interactions (Chiba et al. 2000). Analysis of microbially-derived methane in Iheya North hydrothermal fluids confirmed that the chemical composition is clearly affected by microbial activity (Kawagucci et al. 2011), and fluid flows in turn influence the structure and activity of microbial populations (Yanagawa et al. 2014). The potential microbial community stratification and transition in sub-seafloor sediment cores from Iheya North are controlled by the fluid flow and the geothermal gradient (Yanagawa et al. 2014). Microbial populations in the upper sediment layer are mainly composed of *Chloroflexi* and the deep-sea archaeal group, while microbes in the deeper layer are dominated by archaeal lineages, specifically marine group I, crenarchaeotic and/or euryarchaeotic groups (Yanagawa et al. 2014). Therefore, there exist close relationships between hydrothermal fluids, sediments, and microbial communities. Several studies on the microbial composition of deep-sea sediments in Iheya North have been reported (Wang and Sun 2016; Yanagawa et al. 2013, 2014; Zhang et al. 2015), but very little information on the microbial communities inhabiting the sediments in Iheya Ridge is available.

Microorganisms inhabiting extreme environments have developed numerous mechanisms to deal with the harsh conditions that include high pressure and temperature, extreme acidity and alkalinity, high salinity, and metal toxicity (Pikuta et al. 2007). Genomic analyses of extremophiles have provided some clues to their strategies for surviving in specific niches (Takami et al. 2000, 2002, 2004). In the current study, in order to better understand the environmental adaption mechanisms of the microbes inhabiting the surroundings of deep-sea hydrothermal fields of mid-Okinawa Trough, we performed for the first time a comparative metagenomic analysis of four microbial communities in sediments collected from different distances from vents surrounding Iheya North and Iheya Ridge.

## Materials and methods

### Sample collection

Samples used in this study were collected in April, 2014 during a cruise conducted by the scientific research vessel KEXUE in Okinawa Trough (Wang and Sun 2016). Sediment samples were collected from Iheya hydrothermal fields using an electro hydraulic grabber equipped with an underwater television camera, or a gravity corer. Samples INT4 (126°53.49′E, 27°47.25′N; 1028 m) and INT6 (126°54.32′E, 27°48.47′N; 1190 m) were located at 0.62 km and 2.09 km, respectively, from the hydrothermal vents in Iheya North, while samples IRT2 (126°58.52′E, 27°32.76′N; 1240 m) and IRS6 (126°52.81′E, 27°38.19′N; 1512 m) were located at 0.70 and 13.04 km, respectively, from the hydrothermal vents in Iheya Ridge (Wang and Sun 2016). The ambient temperature of the sampling locations was ~3 °C. The samples were stored at −80 °C and kept on dry ice during transportation.

### Chemical analysis

The chemical composition of the samples was analyzed by the Research Center of Analysis and Measurement, Institute of Oceanology, Chinese Academy of Sciences. The details of sample processing have been described previously (Sun et al. 2015; Zhang et al. 2015). Major metal elements were analyzed by inductively coupled plasma atomic emission spectroscopy (Perkin Elmer, USA) using the strong acid digestion method (Lee et al. 2006).

### DNA extraction

For each surface sediment (upper 10 cm layer), 0.3 g was used for genomic DNA extraction with a TIANamp Soil DNA Kit (Tiangen, Beijing, China). Agarose gel electrophoresis was used to analyze DNA degradation and potential contamination. A NanoPhotometer spectrophotometer (IMPLEN, CA, USA) and a Qubit dsDNA Assay Kit were used to determine DNA purity and concentration, respectively.

### Library construction

One microgram of DNA per sample was used for library construction. A NEBNext Ultra DNA Library Prep Kit for Illumina (NEB, USA) was used to generate 300 bp sequencing libraries according to the manufacturer's recommendations. Briefly, 1 μg of metagenomic DNA was fragmented by sonication to generate ~300 bp fragments that were end-repaired, A-tailed, and ligated with full-length adaptors for further PCR amplification. PCR products were purified using an AMPure XP system, and libraries were analyzed for size distribution with an Agilent 2100 Bioanalyzer and quantified using real-time PCR.

### Metagenomic sequencing and annotation

Metagenomic sequencing was performed using an Illumina HiSeq 2500 platform (Illumina, USA) in Novogene (Tianjin, China). Paired-end raw reads were generated after sequencing, and clean data were extracted from raw reads with the help of quality control processes that removed adaptor fragments and low quality reads. The details of sequence assembly, taxonomic analysis of scaftigs, and annotation of genes have been reported previously (Wang and Sun 2016).

### Phylogenetic analysis

Phylogentic trees were constructed with Neighbor-Joining method in MEGA 6 (Tamura et al. 2013), and bootstrap values were based on percentages of 1000 replicates.

### Accession number

Metagenome datasets have been deposited at the NCBI Sequence Read Archive (http://www.ncbi.nlm.nih.gov/Traces/sra/) under the Accession Number SRP066129.

## Results

Using an Illumina-based sequencing approach, we obtained 85–91 million raw sequences per sample after quality control (data size: ~11G/sample) (Wang and Sun 2016). A total of 287,723, 84,399, 63,015, and 65,481 unique genes were predicted in the metagenomes of INT4, INT6, IRS6, and IRT2 respectively (Wang and Sun 2016). Transposase-encoding genes were detected in all four metagenomes, with relative abundances of 0.16, 0.44, 0.49, and 0.52% in INT4, INT6, IRS6, and IRT2, respectively. Clustering analysis based on functional genes showed that INT6 and IRS6 clustered together, whereas INT4 and IRT2 formed two distinct branches separated from each other and from that formed by INT6 and IRS6 (Fig. 1). Comparison of the four metagenomic datasets was conducted, with a focus on the genes potentially involved in microbial adaptation to deep-sea sediment environments surrounding hydrothermal vents. These genes include those associated with phospholipids and poly-gamma-glutamate (PGA) synthesis, polyamine biosynthesis, $K^+$ influx and efflux, glycine betaine biosynthesis and transport, proline and trehalose biosynthesis, pH and $Na^+$ homeostasis, mechanosensitive channels, and heavy-metal pumps, which have been reported to be involved in microbial adaptations to deep-sea and other harsh environments (Candela and Fouet 2006; Dibrova et al. 2015; Epstein 1986; Fang et al. 2000; Krulwich and Guffanti 1989; Rensing et al. 1997; Romantsov et al. 2009; Silver 1996; Sleator and Hill 2001; Slonczewski et al. 2009; Strøm et al. 1986; Takaki et al. 2010). The relative abundances of these genes in the four samples were shown in Fig. S1.

### Genes associated with phospholipids and poly-gamma-glutamate (PGA) synthesis

Genes *pgsA, pgpA*, and *cls*, encoding phosphatidylglycerophosphate (PGP) synthase (EC 2.7.8.5), PGP phosphatase (EC 3.1.3.27), and cardiolipin synthase (EC 2.7.8.41), respectively, are involved in the formation of phosphatidylglycerol (PG) and cardiolipin (CL). They were found in the four metagenomes. The relative abundance of *pgsA* was ~0.04% in each of the four metagenomes (Fig. 2). The relative abundances of *pgpA* in INT4 (0.009%) and IRT2 (0.014%) were lower than and similar to that in INT6 (0.015%) and IRS6 (~0.015%), respectively (Fig. 2). By contrast, *cls* was relatively more abundant in INT4 (0.029%) and IRT2 (0.026%) than in INT6 (0.007%) and IRS6 (0.011%; Fig. 2). Phylogenetic analysis based on the amino acid sequences of Cls indicated that Cls was related to the uncharacterized taxa belonging to *Deltaproteobacteria, Pseudomonadaceae*, and *Gemmatimonadaceae* (Fig. 3). Genes *pssA* and *psd*, which encode phosphatidylserine synthase and phosphatidylserine decarboxylase, respectively, are involved in the synthesis of phosphatidylethanolamine (PE), and both were abundant in all metagenomes, accounting for ~0.023% (Fig. 2). Genes related to capsular poly-gamma-glutamate (PGA) synthesis were also detected in all four metagenomes, with a relatively higher abundance in INT6 (0.0148%) and IRS6 (0.0122%) than in INT4 (0.0061%) and IRT2 (0.0076%). Phylogenetic analysis based on amino acid sequence of PGA synthesis protein encoded by *capA* showed that these sequences in the four metagenomes were closely related to those from the Gram-positive bacteria *Paenibacillaceae* and *Streptomycetaceae*, the Gram-negative bacteria *Nitrosomonadaceae, Caulobacteraceae*, and *Rhizobiales*, and the archaea Candidatus Bathyarchaeota (Fig. 4).

### Genes involved in polyamine biosynthesis and transport

Putrescine and spermidine are the most common polyamines in prokaryotes (Tabor and Tabor 1985), and norspermine and norspermidine are mainly found in hyperthermophiles (Daniel and Cowan 2000; Takaki et al. 2010). In the four metagenomic datasets, we identified three putrescine biosynthesis pathways (I, II, and III), all of which start with arginine (Fig. 5a). Ornithine and agmatine can be directly converted to putrescine by ornithine decarboxylase (*speC*, EC 4.1.1.17) in pathway I and by agmatinase (*speB*, EC 3.5.3.11) in pathway II, respectively (Fig. 5a). In addition,

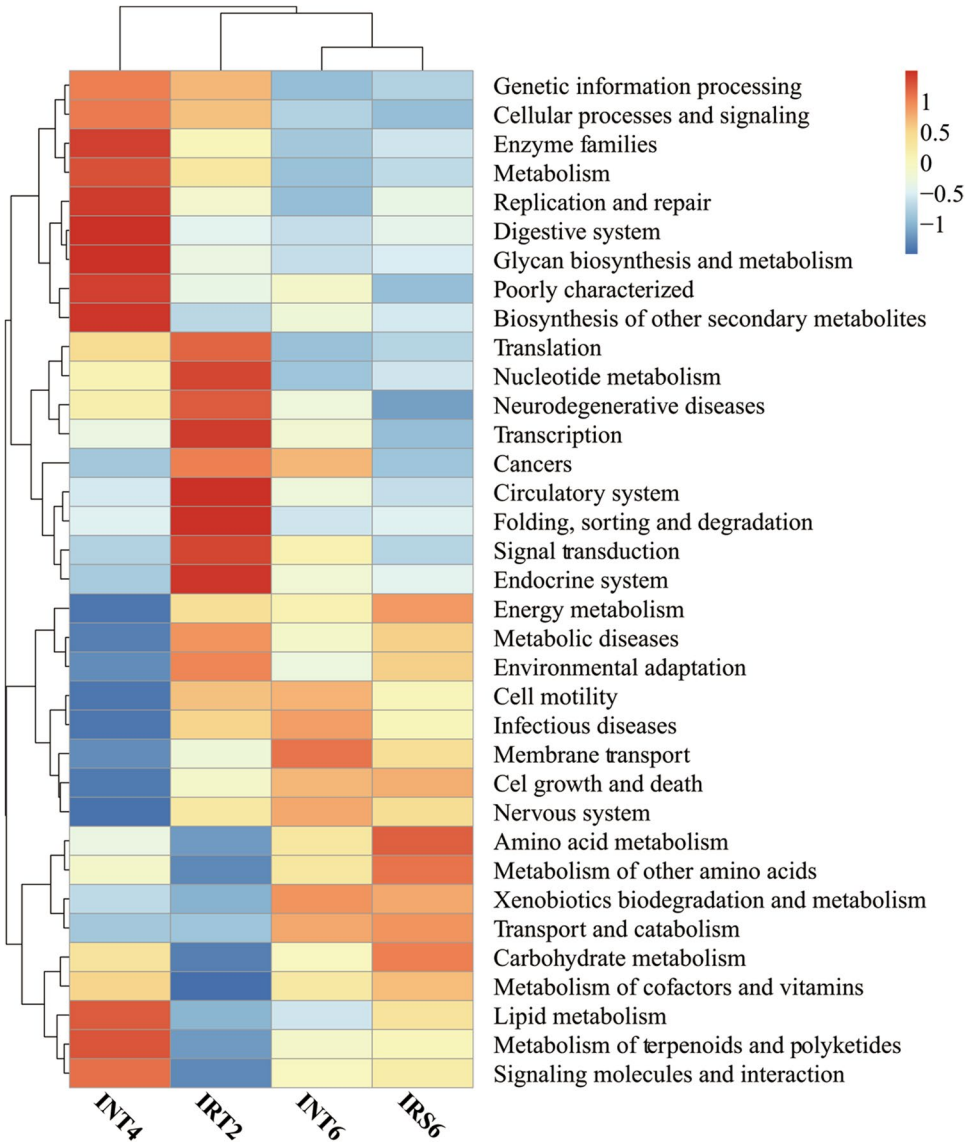


**Fig. 1** Clustering analysis of the microbial communities in the four samples. A total of 35 functional categories that were relatively abundant in the four microbial communities were used to construct the heat-map. The cluster tree is shown on the top, and the relative values of each category among the four samples (*horizontal* clustering) are indicated by *color* intensity on the *right side*. (Color figure online)

agmatine can also be converted to putrescine in two steps via agmatine deiminase (*aguA*, EC 3.5.3.12) and *N*-carbamoylputrescine amidase (*aguB*, EC 3.5.1.53) in pathway III (Fig. 5a). Gene abundance analysis showed that *speB* was relatively more abundant than *speC, aguA*, and *aguB* in every metagenome (Fig. 5b). It is noteworthy that the relative abundances of pathway II genes *speA* (encoding arginine decarboxylase, EC 4.1.1.19) and *speB* were relatively higher in INT6 and IRS6 than in INT4 and IRT2 (Fig. 5b). Spermidine is converted from putrescine by spermidine synthase (*speE*, EC 2.5.1.16) or by the enzymes carboxyspermidine dehydrogenase (CASDH, EC 1.5.1.43) and carboxyspermidine decarboxylase (CASDC, EC 4.1.1.96; Fig. 5a). *speE* was relatively more abundant in INT6 (0.0403%), IRS6 (0.0389%), and IRT2 (0.0400%) than in INT4 (0.0232%; Fig. 5b). By contrast, the gene encoding CASDH was only present in INT4 and IRT2 (relative abundance ~0.0004%), and the gene encoding CASDC (*nspC*) was relatively more abundant in INT4 (0.0046%) and IRT2 (0.0087%) than in INT6 (0.0004%) and IRS6 (0.0014%; Fig. 5b). Spermidine is finally degraded by spermidine $N^1$-acetyltransferase (*speG*, EC 2.3.1.57; Fig. 5a), and *speG* was detected in INT4 (0.0002%), INT6 (0.0020%), and IRS6 (0.0003%) but not in IRT2 (Fig. 5b).

In addition to biosynthesis of polyamines from arginine and methionine, cytoplasmic polyamines can also originate from the surrounding environment via polyamine uptake systems (Fig. 5a). These systems include spermidine/putrescine ATP-binding cassette (ABC) transport system, PotABCD (a spermidine-preferential system), and PotGHIF (a putrescine-specific system) (Igarashi et al. 2001; Kashiwagi et al. 1996). Genes encoding spermidine/putrescine ABC transport systems were more abundant than those encoding PotABCD and PotGHIF systems in all four

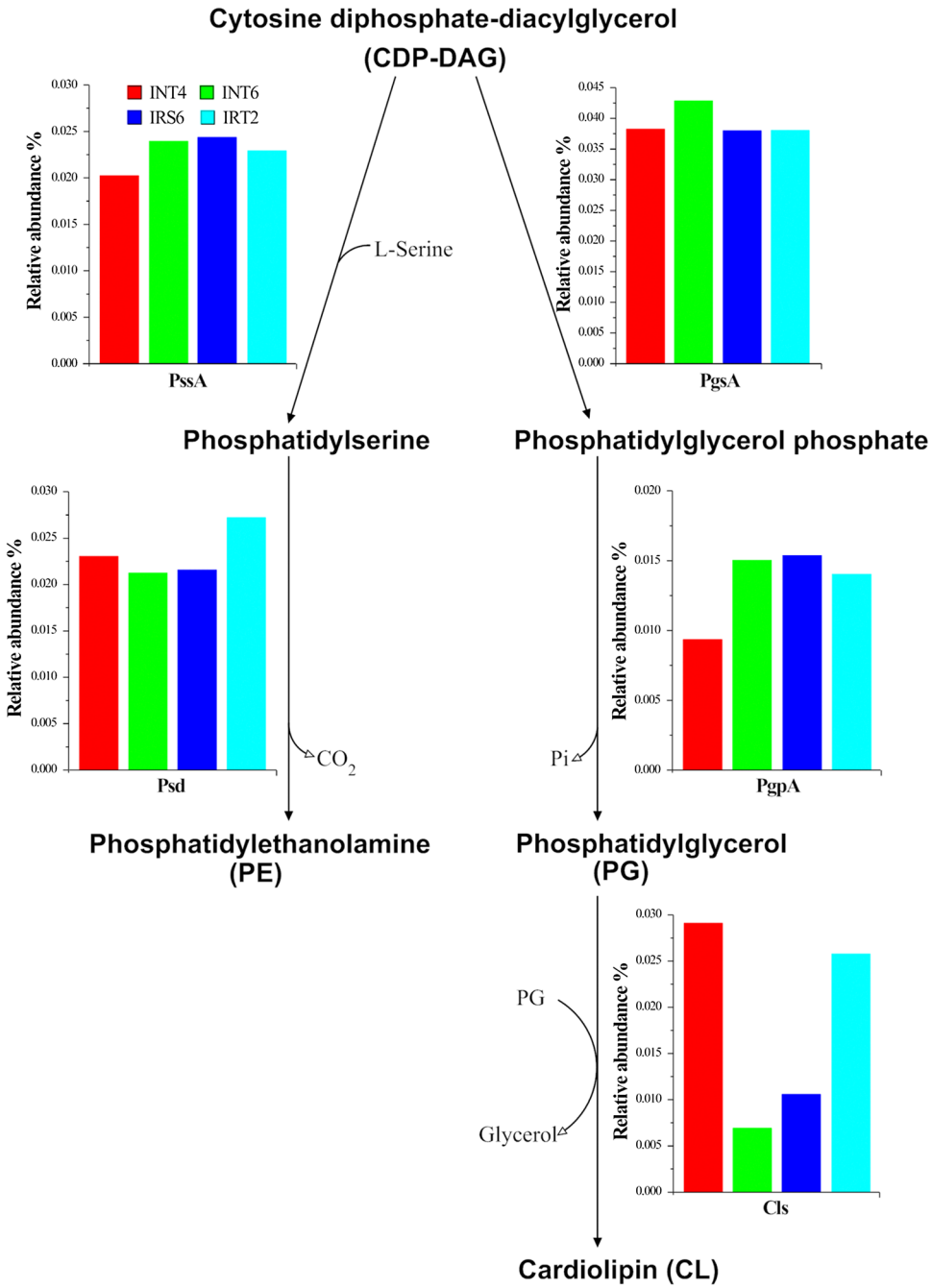


**Fig. 2** Bacterial membrane phospholipid synthesis pathways. *PgsA* phosphatidylglycerophosphate (PGP) synthase, *PgpA* PGP phosphatase, *Cls* cardiolipin synthase, *PssA* phosphatidylserine synthase, *Psd* phosphatidylserine decarboxylase. *Bars* represent the relative abundances of the genes of the pathways

metagenomes (Fig. 5c). The relative abundances of these genes were higher in INT6 and IRS6 than in INT4 and IRT2 (Fig. 5c). Genes involved in antiport systems (e.g., arginine/ornithine antiporter, arginine/agmatine antiporter, and basic amino acid/polyamine antiporter) and polyamine efflux systems (spermidine export system) were also present in all metagenomes (Fig. 5a, c). These may function to expel the substrates (arginine, ornithine, and agmatine) and products (putrescine and spermidine) of polyamine biosynthesis. In every metagenome, especially INT4 and IRT2, the abundances of the genes encoding basic amino acid/polyamine antiporters (TC.APA) were relatively higher than that of the genes encoding other antiport systems (ArcD and AdiC) (Fig. 5c).

### Genes involved in $K^+$ influx and efflux systems

In prokaryotes, $K^+$ is essential for turgor pressure homeostasis and salt tolerance (Nakamura et al. 1998). $K^+$ uptake systems include Kdp, Trk (TrkA-TrkH and TrkG-TrkH complexes), and Kup (Domene and Furini 2012; Nakamura et al. 1998). The most well characterized

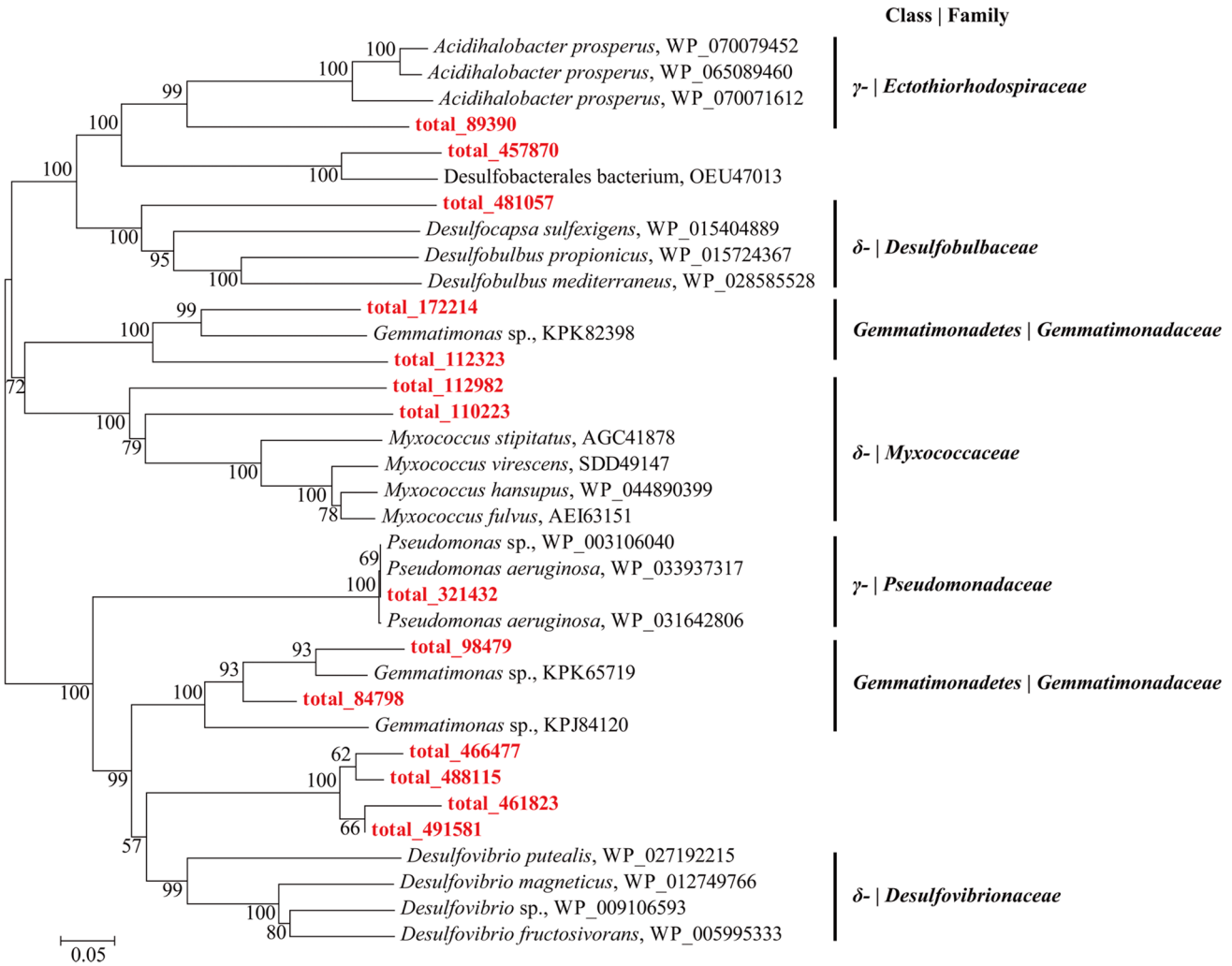


**Fig. 3** Phylogenetic analysis of cardiolipin synthase encoded by *cls*. The tree was constructed using Neighbor-Joining method. Bootstrap values are shown as percentages of 1000 bootstrap replicates. Sequences from this study are in *red*. The *scale bar* represents 0.05 amino acid substitutions per site. γ and δ represent the classes *Gamma-* and *Deltaproteobacteria*, respectively. (Color figure online)

efflux system is the Kef system (Roosild et al. 2002). In our study, Trk was the most dominant $K^+$ uptake system, encoded by *trkA* and *trkH* (Fig. 6). The relative abundances of *trkA* and *trkH* varied from 0.0378 to 0.0516% in the four metagenomes. Next in abundance was the Kup system, which was also present in all metagenomes, with a relative abundance of 0.0053, 0.0035, 0.0020, and 0.0024% in INT4, INT6, IRS6, and IRT2, respectively (Fig. 6). However, the Kdp system was present in INT4, INT6, and IRS6, but not in IRT2 (Fig. 6), with a relative abundance of 0.0007, 0.0070, and 0.0012% in INT4, INT6, and IRS6, respectively. Genes encoding the Kef $K^+$ efflux system were present in the four metagenomes (Fig. 6). The relative abundances of *kefBCG* were 0.0042, 0.0050, 0.0049, and 0.0124% in INT4, INT6, IRS6, and IRT2, respectively (Fig. 6). These genes were most abundant in IRT2.

## Genes involved in glycine betaine biosynthesis and transport systems

In prokaryotes, glycine betaine is a preferred compatible solute among organic osmoprotectants (Sleator and Hill 2001). In *Escherichia coli*, glycine betaine is converted from choline and betaine aldehyde via the osmotically regulated Bet system (Strøm et al. 1986). The Bet system consists of a high-affinity uptake system for choline (BetT), a choline dehydrogenase (BetA), a betaine aldehyde dehydrogenase (BetB), and a regulatory protein (BetI) (Lamark et al. 1992). In this study, genes of the Bet system were found in all four metagenomes (Fig. 7a), but were strikingly more abundant in INT6 and IRS6 than in INT4 and IRT2 (Fig. 7a). Glycine betaine can also accumulate via the ProU and OpuD uptake systems. The ProU system, a multicomponent ABC transport system with a much higher affinity

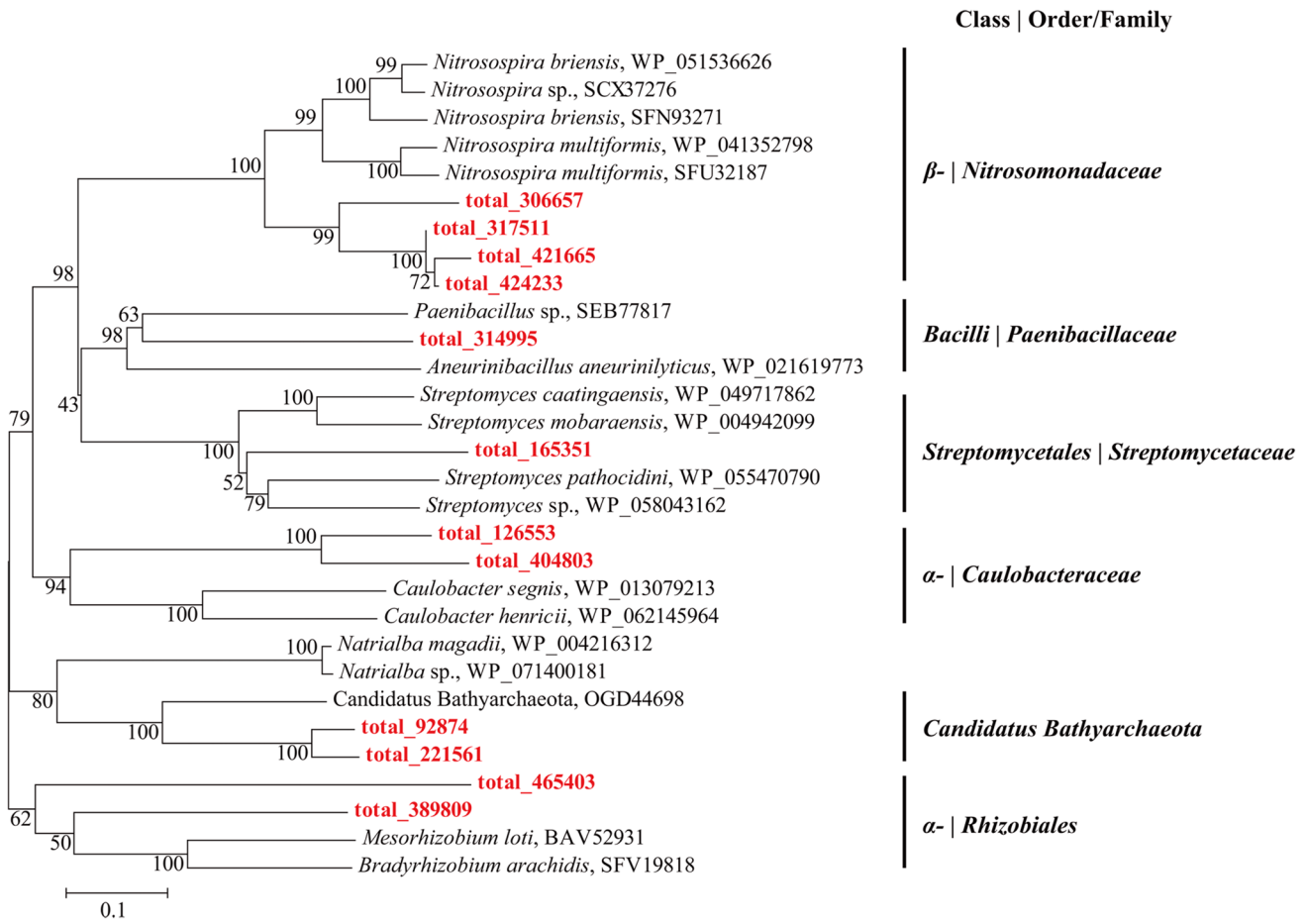


**Fig. 4** Phylogenetic tree based on amino acid sequences of *capA* encoding the poly-gamma-glutamate synthesis protein. The tree was constructed using Neighbor-Joining method. Bootstrap values are shown as percentages of 1000 bootstrap replicates. Sequences from this study are in *red*. The *scale bar* represents 0.1 amino acid substitutions per site. α and β represent the classes *Alpha-* and *Betaproteobacteria*, respectively. (Color figure online)

for glycine betaine than proline, contains two cytoplasmic membrane-bound proteins (ProV and ProW) and one periplasmic binding protein (ProX) (Sleator and Hill 2001), whereas OpuD, encoded by *opuD*, is a single-component transporter (Sleator and Hill 2001). In our study, ProU system genes were abundant in the four metagenomic datasets (Fig. 7b), and genes for both ProU and OpuD systems were more abundant in INT6 and IRS6 than in INT4 and IRT2 (Fig. 7b). In general, the relative abundance of *opuD* was much lower than that of *proX, proW*, and *proV* in every metagenome (Fig. 7b).

### Genes involved in proline biosynthesis

In bacteria, proline can be synthesized via two pathways, from glutamate or ornithine (Sans et al. 1988; Sleator and Hill 2001). In our study, we identified both pathways in the four microbial communities. Genes encoding glutamate 5-kinase, glutamate-5-semialdehyde dehydrogenase, pyrroline-5-carboxylate reductase, and ornithine cyclodeaminase were detected in the four metagenomes (Fig. 8), and their relative abundances were higher in INT6 and IRS6 than in INT4 and IRT2 (Fig. 8).

### Genes involved in trehalose biosynthesis

Trehalose as a cytoplasmic osmolyte accumulates in bacteria under osmotic stress (Strøm et al. 1986). Four trehalose biosynthesis pathways have been identified in prokaryotes, namely OtsA-OtsB, TreT, TreY-TreZ, and TreS, encoded by *otsAB, treT, treYZ*, and *treS*, respectively (Kouril et al. 2008). In this study, all four pathways were identified in the four metagenomes. The genes *otsA* and *otsB* were most abundant, followed by *treT* (Fig. 9). The relative abundances of *otsA* and *otsB* were markedly higher in INT6 and IRS6 than in INT4 and IRT2. However, the opposite was true of *treT* (Fig. 9). Compared to *otsA* and *otsB*, the

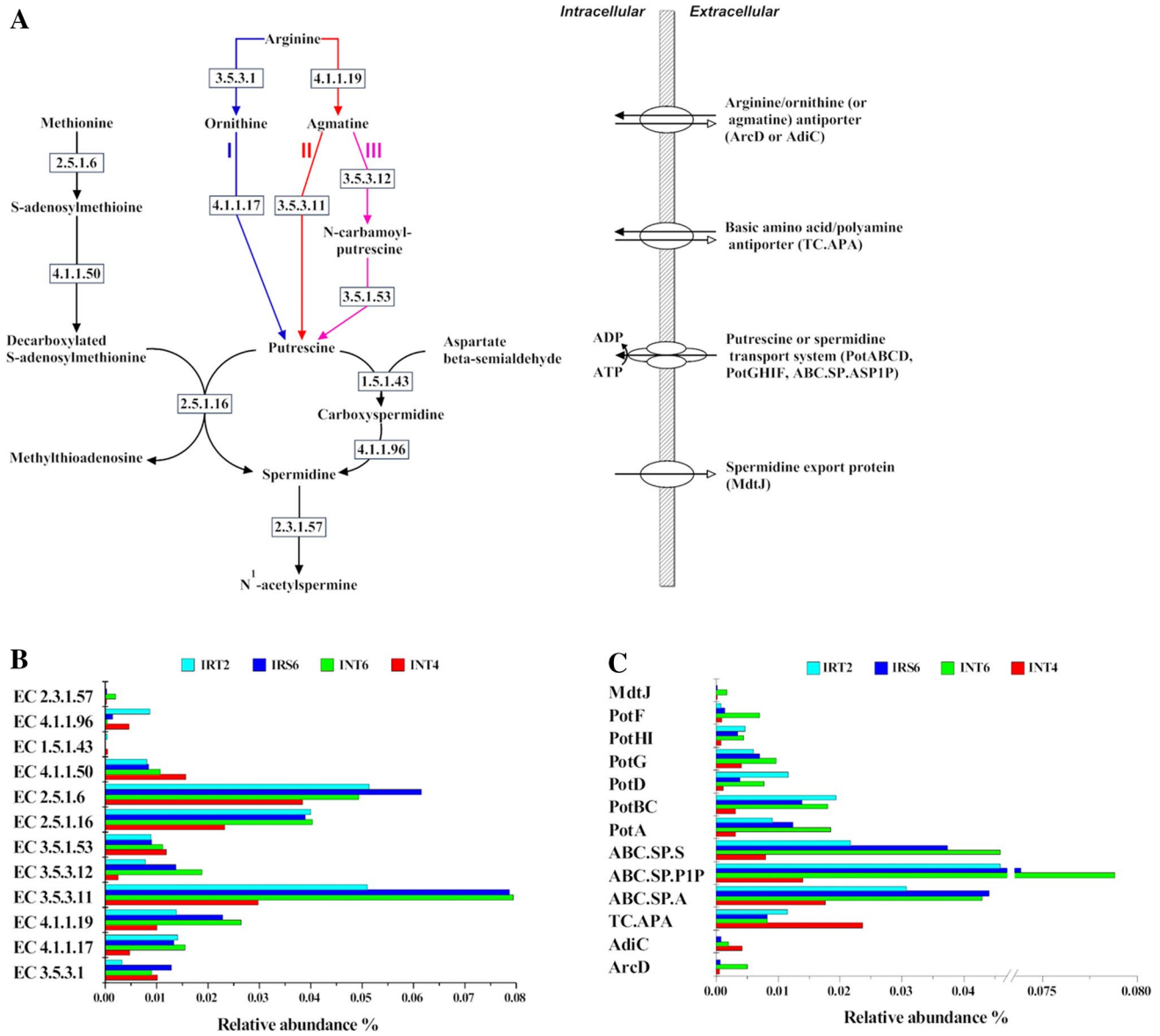


**Fig. 5** Polyamine metabolism. **a** Polyamine biosynthesis and transport systems. The EC numbers of enzymes involved in the synthesis of polyamines are boxed. *Blue, red, and purple arrowed lines* indicate putrescine biosynthesis pathways I, II, and III respectively. Various membrane-spanning transporters participating in the influx and efflux of polyamines are indicated on the *right*. **b** Relative abundances of genes encoding the enzymes involved in polyamine metabolism. EC 3.5.3.1, arginase (*rocF*); EC 4.1.1.17, ornithine decarboxylase (*speC*); EC 4.1.1.19, arginine decarboxylase (*speA*); EC 3.5.3.11, agmatinase (*speB*); EC 3.5.3.12, agmatine deiminase (*aguA*); EC 3.5.1.53, N-carbamoylputrescine amidase (*aguB*); EC 2.5.1.16, spermidine synthase (*speE*); EC 2.5.1.6, *S*-adenosylmethionine synthetase (*metK*); EC 4.1.1.50, *S*-adenosylmethionine decarboxylase (*speD*); EC 1.5.1.43, carboxyspermidine dehydrogenase; EC 4.1.1.96, carboxyspermidine decarboxylase (*nspC*); EC 2.3.1.57, spermidine $N^1$-acetyltransferase (*speG*). **c** Relative abundances of genes encoding transporters of polyamine transport systems. (Color figure online)

abundances of *treY, treZ*, and *treS* were much lower in all four metagenomes (Fig. 9).

## Mechanosensitive channel genes

Mechanosensitive channels (MSCs) are major routes for the release of cytoplasmic solutes, and their function helps to achieve a rapid reduction in the turgor pressure in response to a rapid decrease in external osmolarity (Berrier et al. 1992). In bacteria, two MSCs have been cloned and crystallized: the large conductance channel MscL (Chang et al. 1998; Sukharev et al. 1994) and the small conductance channel MscS (Bass et al. 2002; Levina et al. 1999). In our study, *mscS* was much more abundant than *mscL* in every metagenome (Fig. 10). In

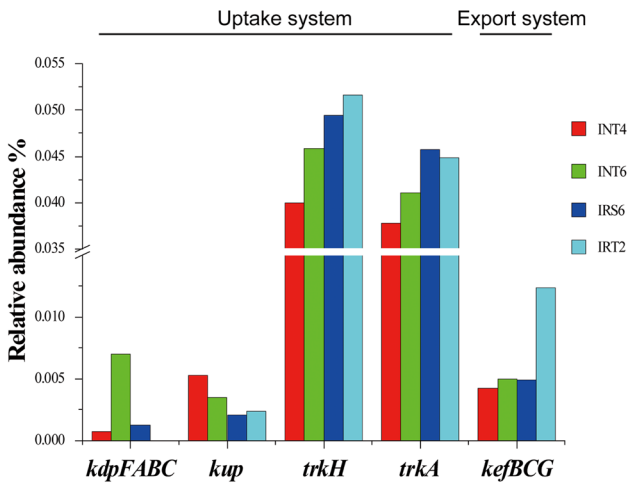


**Fig. 6** Relative abundances of genes encoding potassium ion uptake and efflux systems. *kdpFABC*, encoding $K^+$-transporting ATPase (among P-type ATPase family); *kup*, encoding $K^+$ uptake protein of Kup system; *trkA* and *trkH*, encoding $K^+$ uptake proteins TrkA and TrkH of Trk system; *kefBCG*, encoding glutathione-regulated $K^+$ efflux (Kef) system

addition, the abundances of *mscS* in INT6 and IRS6 were higher than that in INT4 and IRT2 (Fig. 10).

### Genes involved in pH homeostasis

In deep-sea sediments enriched with organic matters, maintaining an optimal pH is essential to intracellular enzyme activities and physiological processes. Proton entry and efflux are critical for intracellular pH homeostasis, which use primary proton pumps such as $H^+$-coupled ATPases, and secondary transporters such as cation/proton antiporters (Hunte et al. 2005; Janto et al. 2011; Krulwich et al. 2011; Slonczewski et al. 2009). In this study, various cation ($Na^+$, $K^+$, and $Ca^{2+}$)/proton antiporters, proton-exporting ATPase, $F_1F_o$-ATPase, and the proton/glutamate symporter were detected in every metagenome (Fig. 11). These transport systems are responsible for the entry and efflux of protons in exchange with cations. Genes of the *atp* operon encoding $F_1F_o$-ATPase were abundant in all metagenomes (Fig. 11b). Among the secondary active transporters, the multicomponent $Na^+/H^+$ antiporter was most abundant, followed by monovalent cation/proton antiporter-2 (CPA2), monovalent cation/proton antiporter-1 (CPA1), multicomponent $K^+/H^+$ antiporter, and $Na^+/H^+$ antiporter NhaA (Fig. 11b). The relative abundances of genes encoding $Na^+/H^+$ antiporter NhaB, $Ca^{2+}/H^+$ antiporter ChaA, and proton/glutamate symporter were very low in every metagenome (Fig. 11b). It is noteworthy that the relative abundances of $Na^+/H^+$ antiporter NhaC and proton-exporting ATPase in INT4 and IRT2 were much higher than that in INT6 and IRS6 (Fig. 11b).

### Genes involved in $Na^+$ homeostasis

Genes encoding primary $Na^+$ pumps and $Na^+$-dependent secondary transporters were found in our four metagenomic datasets. The relative abundances of genes encoding inorganic pyrophosphatase and sodium-transporting NADH:ubiquinone oxidoreductase were markedly higher than that of genes encoding the sodium transport system and oxaloacetate decarboxylase (Fig. 12). $Na^+/H^+$ antiporters, mentioned above in reference to pH homeostasis, likely play a dominant role in cytoplasmic $Na^+$ export. Some co-transporting systems, such as the solute/$Na^+$ symporter, neurotransmitter/$Na^+$ symporter, glutamate/$Na^+$ symporter, and phosphate/$Na^+$ symporter (Fig. 12), probably function in $Na^+$ re-entry coupled to solute uptake. The relative abundances of genes encoding the neurotransmitter/$Na^+$ symporter were relatively higher in INT4 and IRT2 than in INT6 and IRS6 (Fig. 12). By contrast, the relative abundances of genes encoding the phosphate/$Na^+$ symporter were higher in INT6 and IRS6 than in INT4 and IRT2 (Fig. 12).

### Genes encoding heavy-metal pumps

The metals Ca, Fe, Mg, Mn, Ba, Cu, Pb, Zn, and As were detected in the four sediments, of which Cu, Pb, and Zn were relatively much more abundant in INT4 and IRT2 (Table S1). In our metagenomic datasets, the genes related to $Cu^{2+}$-exporting and $Cd^{2+}/Zn^{2+}$-exporting ATPases, which are probably involved in pumping Cu, Zn, and/or Cd, were found in all four metagenomes. The relative abundances of these genes were higher in INT4 and IRT2 than in INT6 and IRS6 (Fig. S2). Phylogenetic analysis based on the sequences of $Cd^{2+}/Zn^{2+}$-exporting ATPase showed that they were related to novel uncharacterized taxa belonging to the classes of *Alpha-, Beta-, Gamma-, Zetaproteobacteria, Deinococci*, and *Halobacteria*, and the phyla Nitrospirae and Candidatus N10 (Fig. 13).

## Discussion

### Composition of cell surface structure

The cell surface structure (membrane and cell wall) is essential to the survival of microorganisms in extreme environments. As a survival mechanism, the phospholipid composition of the bacterial membrane, especially the cardiolipin content, can change in response to external stresses (Clejan et al. 1986; Corcelli 2009; Enomoto and Koyama 1999; Romantsov et al. 2007, 2009; Zhang and Rock 2008). In our study, we found that the *cls* gene was more abundant in INT4 and IRT2, which are closer to hydrothermal vents

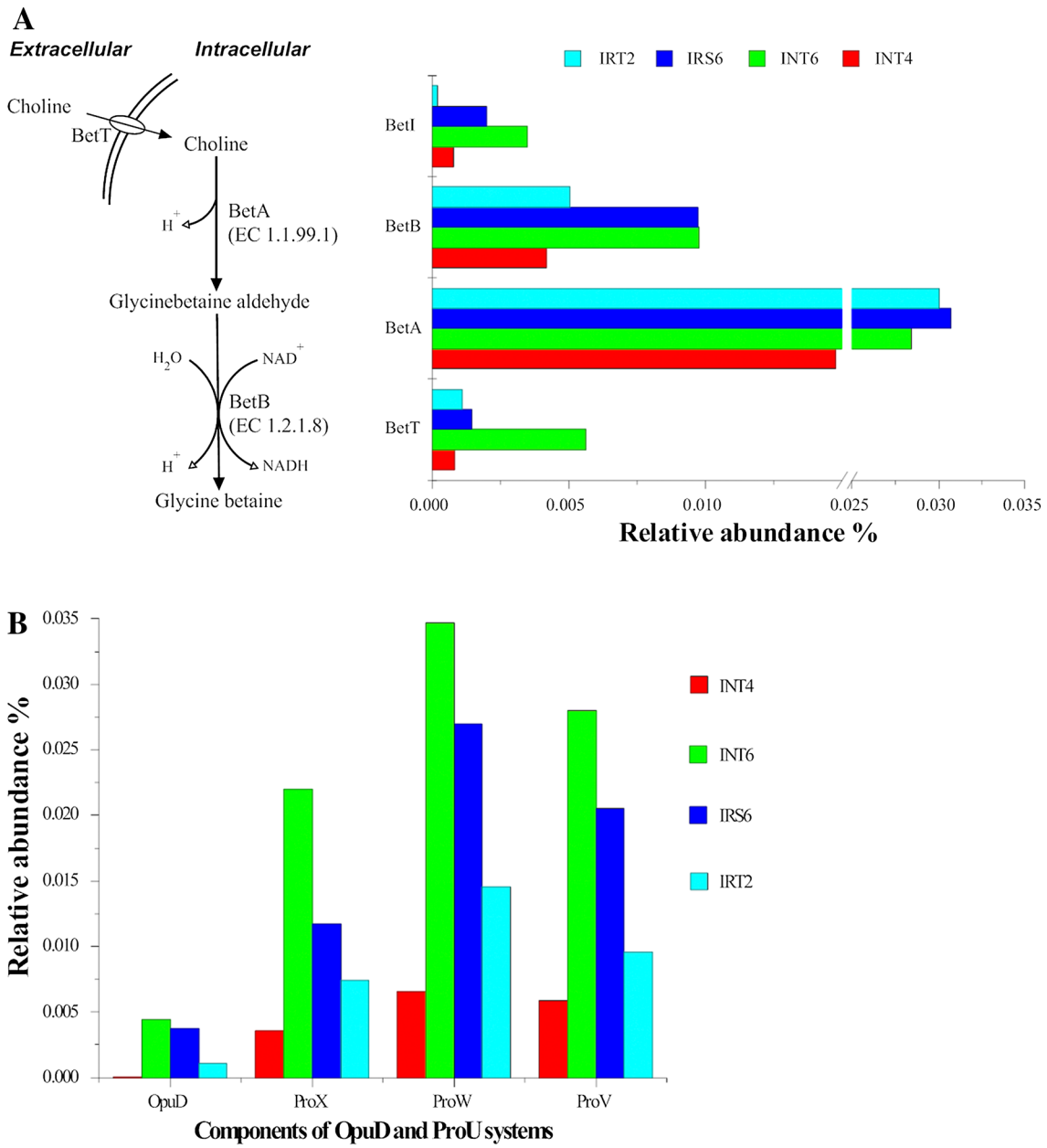


**Fig. 7** Glycine betaine biosynthesis and transport systems. **a** The glycine betaine biosynthesis pathway proceeding via the Bet system using exogenous choline (*left*), and the relative abundances of genes encoding the Bet system (*right*). **b** Relative abundances of genes encoding the glycine betaine uptake systems OpuD and ProU

than INT6 and IRS6, while the *pgpA* gene was more abundant in INT6 and IRS6. These results indicate that the compositions of phospholipids PG and CL varied in the microorganisms from different habitats, and were affected by the distance from hydrothermal vents. Previous reports showed that CL has the potential to act as a proton sink in membranes, and elevated CL facilitates adaptation to higher salinity and pH (Enomoto and Koyama 1999; Haines and Dencher 2002; Lopez et al. 2006; Romantsov et al. 2007, 2009). The relatively higher abundance of CL-encoding gene in the sediments closer to the vent sites suggests that elevating the CL content may serve to enhance proton permeability, thereby contributing to the maintenance of cytoplasmic pH homeostasis, which is likely to be a more challenging task at sites closer to vents.

Phylogenetic analysis showed that in our study, PGA was synthesized by some bacteria, especially Gram-positive bacteria, and by Bathyarchaeota. Bathyarchaeota was recently reported as a novel methanogenic archaeal lineage in deep-ocean and freshwater sediments (Evans et al.

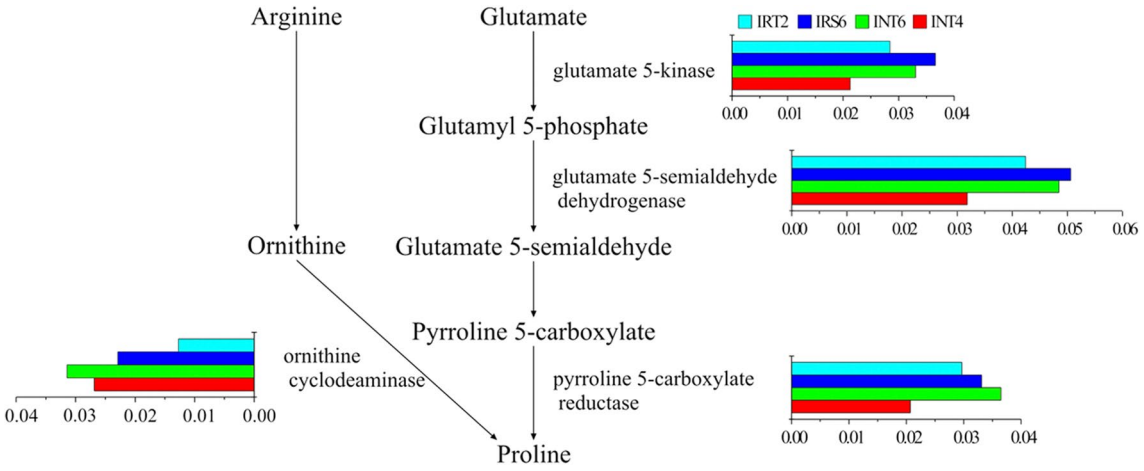


**Fig. 8** Proline synthesis pathways. The two pathways for proline synthesis are indicated. *Bars* represent the relative abundances of genes involved

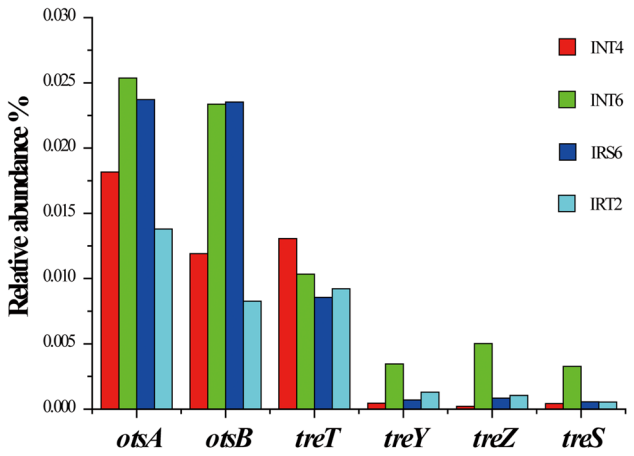


**Fig. 9** Relative abundances of genes involved in trehalose biosynthesis pathways

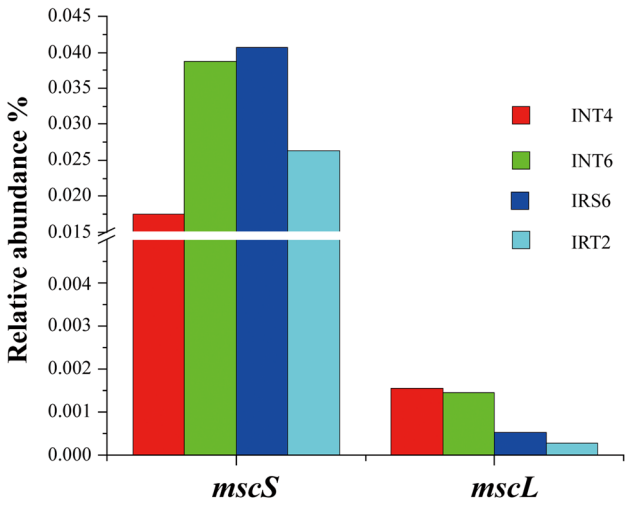


**Fig. 10** Abundance of genes encoding mechanosensitive channels. *mscS*, coding gene of mechanosensitive channel of small conductance; *mscL*, coding gene of mechanosensitive channel of large conductance

2015). The presence of Bathyarchaeota in our samples suggests a possible participation of Bathyarchaeota in methane production in Iheya hydrothermal fields. In addition, PGA can also be synthesized by some chemolithoautotrophs belonging to *Nitrosospira*, which are able to oxidize ammonia (Bock and Wagner 2006). It has diverse physiological functions and plays different roles that enable the organism to adapt to specific environments (Candela and Fouet 2006). Some bacteria use PGA for capsule synthesis, while others use it for the sequestration of metal ions and reducing high local salt concentrations (Hezayen et al. 2001; Kandler et al. 1983; McLean et al. 1990; Uchida et al. 1985). In our study, a higher abundance of PGA-encoding genes was found in INT6 and IRS6 than in INT4 and IRT2, indicating an influence of the proximity to vents in this biological function.

## Polyamine metabolism and homeostasis

In this study, pathway II (via agmatinase) was identified as the major route for putrescine biosynthesis, and is likely to be preferred by microorganisms inhabiting the regions distant from the vents, as indicated by the richness of the *speB* gene in INT6 and IRS6. Spermidine can be directly converted from putrescine by spermidine synthase as a primary biosynthetic route, or indirectly via carboxyspermidine as an alternative route, i.e. the CASDH/CASDC pathway, which is known to be critical for the growth of some bacteria such as *Campylobacter jejuni* (Hanfrey et al. 2011) and *Deferribacter desulfuricans* (Takaki et al. 2010). Given

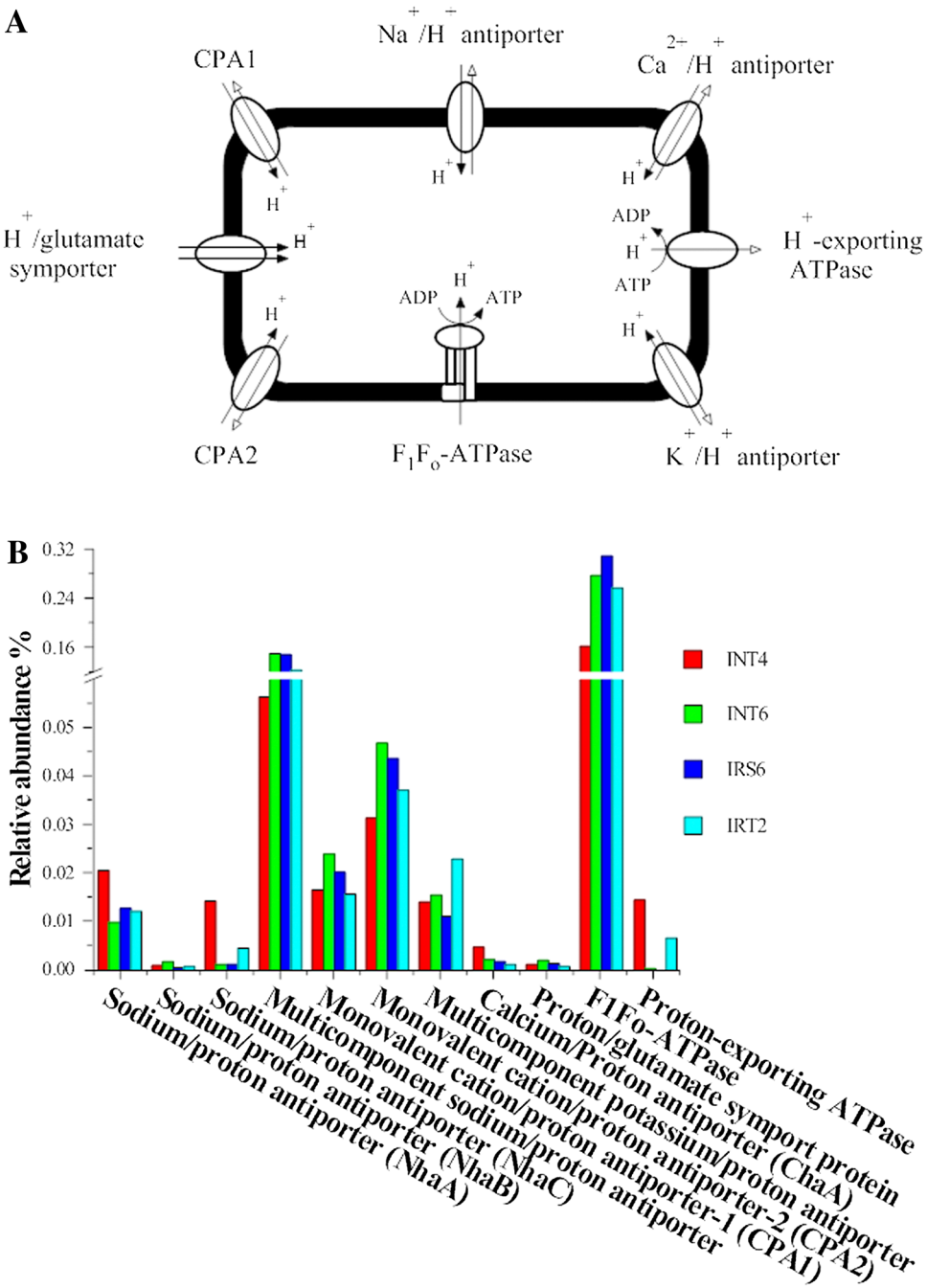


**Fig. 11** pH homeostasis. **a** Transport systems involved in proton influx and efflux. **b** Relative abundances of genes encoding proton-translocating systems

the relatively higher abundance of CASDH- and CASDC-encoding genes in INT4 and IRT2, the CASDH/CASDC biosynthesis pathway probably plays a more important role in the survival of microbial communities closer to vent orifices. The basic amino acid/polyamine antiport system was observed in all four metagenomes in this study. Importing new basic amino acids through this system probably contributes to pH homeostasis in these microbial communities. In addition, carbon dioxide and ammonia, produced during polyamine biosynthesis (Tabor and Tabor 1985), could also participate in intracellular pH regulation. Therefore, polyamine metabolism is probably connected with pH homeostasis in microbes inhabiting the hydrothermal fields of Iheya.

## Osmoadaptation

More $Na^+$ than $K^+$ is contained in marine environments, while it is contrary in the cytoplasm of marine microbes (Dibrova et al. 2015). To maintain a relatively higher concentration of intracellular $K^+$, multiple $K^+$ uptake systems exist in microorganisms. In our study, three $K^+$ uptake

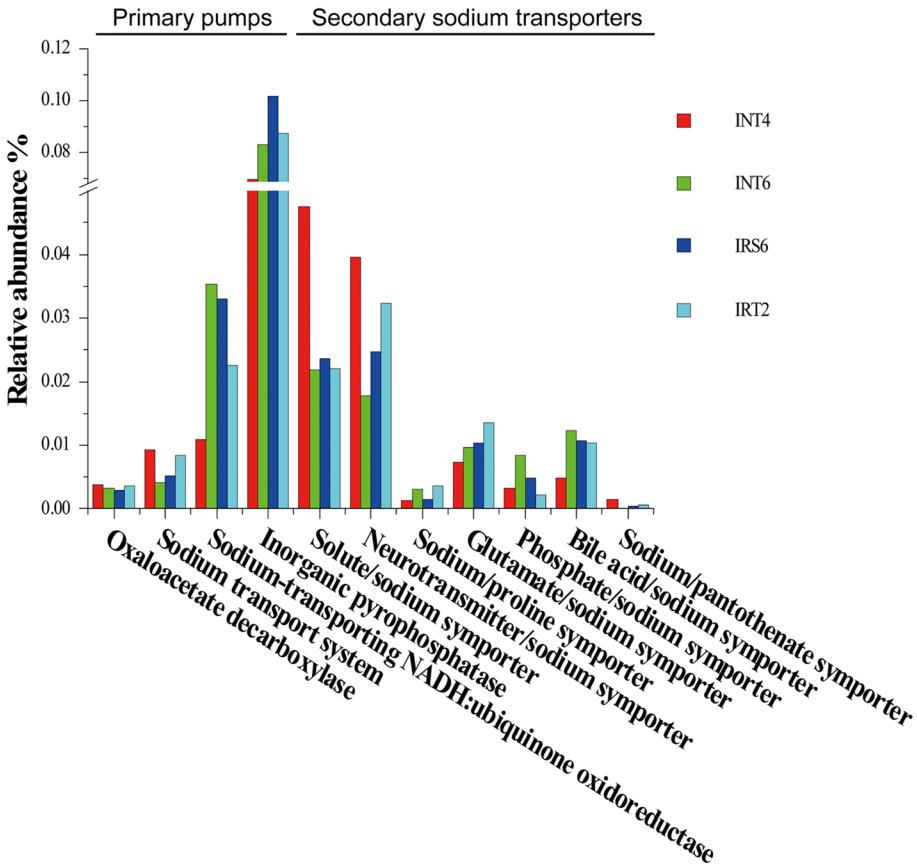


**Fig. 12** Relative abundances of genes encoding sodium transport systems

systems (KdpFABC, Kup, and Trk) were found in the four metagenomes. Of these, the Trk system was the most abundant, presumably due to its low affinity for $K^+$ (Epstein 1986). The Kup system, which has an intermediate affinity for $K^+$ (Nakamura et al. 1998), was the next abundant system. The least abundant $K^+$ uptake system (KdpFABC) is inducible in *E. coli* and has a high affinity for $K^+$ (Epstein 1986). These results support the hypothesis that the low- and intermediate-affinity $K^+$ uptake systems (Trk and Kup) are widely used by the microorganisms at all four sites as 'house-keeping' $K^+$ influx systems, while the high-affinity system (Kdp) was only present in some microbes, possibly as an emergency system that operates when $K^+$ uptake is urgently required.

Under osmotic stress, microorganisms accumulate organic osmolytes together with $K^+$ in their cytoplasm to enhance the internal osmotic strength (Strøm et al. 1986). In the four metagenomic datasets in our study, we identified abundant genes related to the biosynthesis and transport of glycine betaine, proline, and trehalose, which may serve as organic osmolytes and play a role in microbial osmoadaptation. Indeed, previous reports have shown that glycine betaine and proline confer osmoprotection and salt tolerance in bacteria (Ko et al. 1994; Sleator et al. 2001; Strøm et al. 1986), and trehalose protects proteins and membranes from inactivation or denaturation caused by a variety of stresses (Elbein et al. 2003). MSCs (MscL and MscS) are responsible for the rapid release of intracellular solutes in response to osmotic shock to protect cells from lysis (Berrier et al. 1992; Levina et al. 1999). In our study, *mscS* was much more abundant than *mscL* in all metagenomes, suggesting that MscS was likely preferred by the microorganisms in the four sediments, which is in line with the report of Bass et al., who found that MscS has a far greater distribution than MscL throughout bacteria (Bass et al. 2002).

## pH homeostasis

The primary proton pump $F_1F_o$-ATPase was abundant in the four sediments in our study. $F_1F_o$-ATPase generates proton motive force in microorganisms and promotes protons across the membrane (Krulwich et al. 2011). Since greater energy is required to maintain cytoplasmic pH homeostasis and ATP synthesis to support microbial growth at higher pH or under alkaline conditions (Hicks et al. 2010), the abundant $F_1F_o$-ATPase may serve to provide sufficient ATPs for pH regulation in microbes inhabiting hash hydrothermal environments. The richness of $F_1F_o$-ATPase is consistent with the high abundance of multiple cation/proton antiporters, which probably require energy (ATPs)

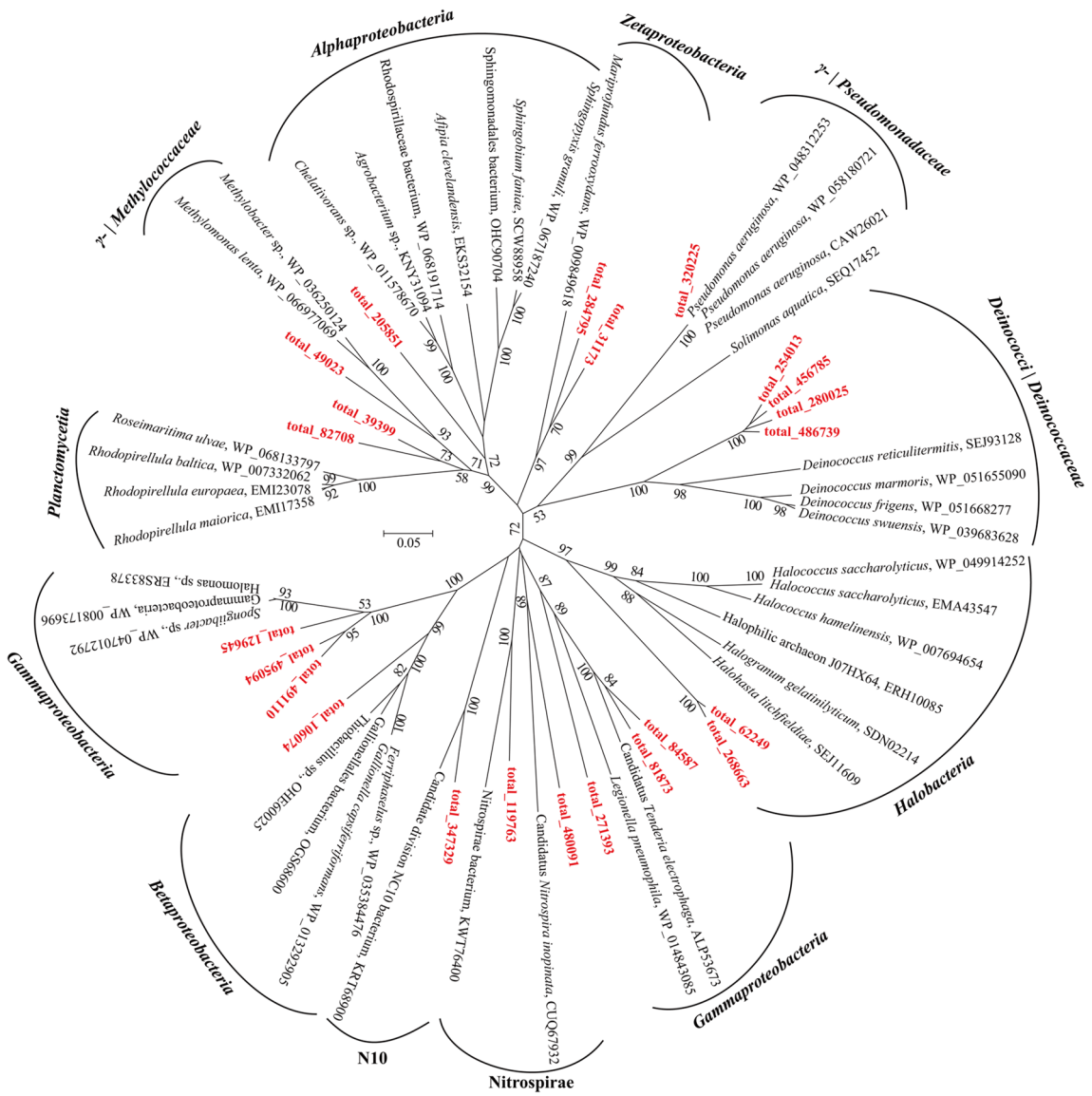


**Fig. 13** Phylogenetic tree based on amino acid sequences of $Cd^{2+}$/$Zn^{2+}$ transporting ATPase. The tree was constructed using Neighbor-Joining method. Bootstrap values are shown as percentages of 1000 bootstrap replicates. Sequences from this study are in *red*. The *scale bar* represents 0.05 amino acid substitutions per site. γ represents the class *Gammaproteobacteria*. (Color figure online)

produced by $F_1F_o$-ATPase. It has also been reported that $Na^+/H^+$ antiporter is energized by the electrochemical proton gradient formed by $F_1F_o$-ATPase (Krulwich and Guffanti 1989).

## $Na^+$ homeostasis

Energy transduction in most bacteria is realized by combining a primary proton pump with the generation of a sodium gradient (Speelmans et al. 1995). There are a variety of $Na^+$ pumps participating in the generation of electrochemical gradient (Dibrova et al. 2015; Krulwich and Guffanti 1989). In the four samples in our study, the dominant primary $Na^+$ export pumps were inorganic pyrophosphatase and $Na^+$-translocating NADH:ubiquinone oxidoreductase, which are independent of proton-motive force (Dibrova et al. 2015). Some solute-sodium co-transport systems (i.e., neurotransmitter/$Na^+$ symporter, solute/$Na^+$ symporter, glutamate/$Na^+$ symporter, and phosphate/$Na^+$ symporter) were likely responsible for $Na^+$ re-entry and functioned as complementary components in $Na^+$ homeostasis.

## Heavy-metal pumps

In this and previous studies, metal elements including the toxic heavy metals Cu, Pb, and Zn were detected in Iheya

North and Iheya Ridge. Consistent with the observation that Cu and Zn were enriched in INT4 and IRT2, the relatively abundances of genes encoding $Cu^{2+}$-exporting ATPase (CopB) and $Cd^{2+}/Zn^{2+}$-exporting ATPase (ZntA) were much higher in INT4 and IRT2 than in INT6 and IRS6. CopB and ZntA are well-characterized metal pumps with a high affinity for $Cu^{2+}$ and $Zn^{2+}$ respectively (Mana-Capelli et al. 2003; Palmgren and Nissen 2011; Rensing et al. 1997). These pumps likely participate in exporting excess heavy-metal ions from the cytoplasm, thereby conferring resistance to copper, zinc, and/or cadmium. In this study, some bacteria containing *zntA* were closely related to *Nitrospira, Methylococcaceae*, and *Mariprofundus*, which are capable of oxidizing ammonia, methane, and $Fe^{2+}$ respectively (Nunes-Alves 2016; Ruff et al. 2015; Singer et al. 2011).

## Conclusion

In this study, we provided the first systematic genetic evidences that microorganisms inhabiting the sediments surrounding hydrothermal vents in Iheya North and Iheya Ridge possess genes involved in a variety of metabolic processes that maintain specific cell surface structure, osmoadaptation, and homeostasis of organic solutes, inorganic ions, and pH. In addition, we observed apparent influences of the distance from hydrothermal vents on the distribution of some of these genes. These results add insight into microbial adaptation mechanisms in deep-sea environments associated with hydrothermal fields.

**Acknowledgements** This work was supported by the grants of the Strategic Biological Resources Service Network Plan and the Strategic Priority Research Program of Chinese Academy of Sciences (ZSSD-005 and XDA11030401) and the Taishan Scholar Program of Shandong Province. We thank the WPOS (Western Pacific Ocean System) sample center for providing the samples.

## References

Bass RB, Strop P, Barclay M, Rees DC (2002) Crystal structure of *Escherichia coli* MscS, a voltage-modulated and mechanosensitive channel. Science 298:1582–1587. doi:10.1126/science.1077945

Berrier C, Coulombe A, Szabo I, Zoratti M, Ghazi A (1992) Gadolinium ions inhibit the loss of metabolites induced by osmotic shock and large stretch-activated channels in bacteria. Eur J Biochem 206:559–565. doi:10.1111/j.1432-1033.1992.tb16960.x

Bock E, Wagner M (2006) Oxidation of inorganic nitrogen compounds as an energy source. In: Dworkin M, Falkow S, Rosenberg E, Schleifer K-H, Stackebrandt E (eds) The prokaryotes, 3rd edn. Springer, New York, pp 457–495

Candela T, Fouet A (2006) Poly-gamma-glutamate in bacteria. Mol Microbiol 60:1091–1098. doi:10.1111/j.1365-2958.2006.05179.x

Chang G, Spencer RH, Lee AT, Barclay MT, Rees DC (1998) Structure of the MscL homolog from *Mycobacterium tuberculosis*: a gated mechanosensitive ion channel. Science 282:2220–2226

Chiba H, Kataoka S, Ishibashi J, Yamananka T (2000) Distribution of hydrothermal vents, fluid chemistry, and phase separation at the Iheya North seafloor hydrothermal system, Mid-Okinawa Trough. EOS Trans Am Geophys Union 81:WP86 (**Abstract**)

Clejan S, Krulwich TA, Mondrus KR, Seto-Young D (1986) Membrane lipid composition of obligately and facultatively alkalophilic strains of *Bacillus* spp. J Bacteriol 168:334–340

Corcelli A (2009) The cardiolipin analogues of Archaea. Biochim Biophys Acta 1788:2101–2106. doi:10.1016/j.bbamem.2009.05.010

Daniel RM, Cowan DA (2000) Biomolecular stability and life at high temperatures. Cell Mol Life Sci 57:250–264. doi:10.1007/PL00000688

Dibrova DV, Galperin MY, Koonin EV, Mulkidjanian AY (2015) Ancient systems of sodium/potassium homeostasis as predecessors of membrane bioenergetics. Biochemistry (Moscow) 80:495–516. doi:10.1134/S0006297915050016

Domene C, Furini S (2012) Molecular dynamics simulations of the TrkH membrane protein. Biochemistry 51:1559–1565. doi:10.1021/bi201586n

Elbein AD, Pan YT, Pastuszak I, Carroll D (2003) New insights on trahalose: a multifunctional molecule. Glycobiology 13:17R–27R. doi:10.1093/glycob/cwg047

Enomoto K, Koyama N (1999) Effect of growth pH on the phospholipid contents of the membranes from alkaliphilic bacteria. Curr Microbiol 39:270–273

Epstein W (1986) Osmoregulation by potassium transport in *Escherichia coli*. FEMS Microbiol Lett 39:73–80. doi:10.1016/0378-1097(86)90063-7

Evans PN, Parks DH, Chadwick GL, Robbins SJ, Orphan VJ, Golding SD, Tyson GW (2015) Methane metabolism in the archaeal phylum Bathyarchaeota revealed by genome-centric metagenomics. Science 350:434–438. doi:10.1126/science.aac7745

Fang JS, Barcelona MJ, Nogi Y, Kato C (2000) Biochemical implications and geochemical significance of novel phospholipids of the extremely barophilic bacteria from the Marianas Trench at 11,000 m. Deep-Sea Res I(47):1173–1182. doi:10.1016/S0967-0637(99)00080-1

Gamo T, Sakai H, Kim ES, Shitashima K, Ishibashi J (1991) High alkalinity due to sulfate reduction in the CLAM hydrothermal field, Okinawa Trough. Earth Planet Sci Lett 107:328–338

Glasby GP, Notsu K (2003) Submarine hydrothermal mineralization in the Okinawa Trough, SW of Japan: an overview. Ore Geol Rev 23:299–339. doi:10.1016/j.oregeorev.2003.07.001

Haines TH, Dencher NA (2002) Cardiolipin: a proton trap for oxidative phosphorylation. FEBS Lett 588:35–39. doi:10.1016/S0014-5793(02)03292-1

Hanfrey CC, Pearson BM, Hazeldine S, Lee J, Gaskin DJ, Woster PM, Phillips MA, Michael AJ (2011) Alternative spermidine biosynthetic route is critical for growth of *Campylobacter jejuni* and is the dominant polyamine pathway in human gut microbiota. J Biol Chem 286:43301–43312. doi:10.1074/jbc.M111.307835

Hezayen FF, Rehm BH, Tindall BJ, Steinbüchel A (2001) Transfer of *Natrialba asiatica* B1T to *Natrialba taiwanensis* sp. nov. and description of *Natrialba aegyptiaca* sp. nov., a novel extremely halophilic, aerobic, non-pigmented member of the Archaea from Egypt that produces extracellular poly(glutamic acid). Int J Syst Evol Microbiol 51:1133–1142. doi:10.1099/00207713-51-3-1133

Hicks DB, Fujisawa M, Krulwich TA (2010) $F_1F_o$-ATP synthases of alkaliphilic bacteria: lessons from their adaptations. Biochim Biophys Acta 1797:1362–1377. doi:10.1016/j.bbabio.2010.02.028

Hunte C, Screpanti E, Venturi M, Rimon A, Padan E, Michel H (2005) Structure of a $Na^+/H^+$ antiporter and insights into mechanism of action and regulation by pH. Nature 435:1197–1202. doi:10.1038/nature03692

Igarashi K, Ito K, Kashiwagi K (2001) Polyamine uptake systems in *Escherichia coli*. Res Microbiol 152:271–278. doi:10.1016/S0923-2508(01)01198-6

Janto B, Ahmed A, Ito M, Liu J, Hicks DB, Pagni S, Fackelmayer OJ, Smith TA, Earl J, Elbourne LD, Hassan K, Paulsen IT, Kolstø AB, Tourasse NJ, Ehrlich GD, Boissy R, Ivey DM, Li G, Xue Y, Ma Y, Hu FZ, Krulwich TA (2011) The genome of alkaliphilic *Bacillus pseudofirmus* OF4 reveals adaptations that support the ability to grow in an external pH range from 7.5 to 11.4. Environ Microbiol 13:3289–3309. doi:10.1111/j.1462-2920.2011.02591.x

Kandler O, KÓ§nig H, Wiegel J, Claus D (1983) Occurrence of poly-γ-D-glutamic acid and poly-α-L-glutamine in the genera *Xanthobacter, Flexithrix, Sporosarcina* and *Planococcus*. Syst Appl Microbiol 4:34–41. doi:10.1016/S0723-2020(83)80032-0

Kashiwagi K, Pistocchi R, Shibuya S, Sugiyama S, Morikawa K, Igarashi K (1996) Spermidine-preferential uptake system in *Escherichia coli*: identification of amino acids involved in polyamine binding in PotD protein. J Biol Chem 271:12205–12208. doi:10.1074/jbc.271.21.12205

Katayama H, Watanabe Y (2003) The Huanghe and Changjiang contribution to seasonal variability in terrigenous particulate load to the Okinawa Trough. Deep Sea Res Part II 50:475–485. doi:10.1016/S0967-0645(02)00469-1

Kawagucci S, Chiba H, Ishibashi JI, Yamanaka T, Toki T, Muramatsu Y, Ueno Y, Makabe A, Inoue K, Yoshida N, Nakagawa S, Nunoura T, Takai K, Takahata N, Sano Y, Narita T, Teranishi G, Obata H, Gamo T (2011) Hydrothermal fluid geochemistry at the Iheya North field in the mid-Okinawa Trough: implication for origin of methane in subseafloor fluid circulation systems. Geochem J 45: 109–124. doi:10.2343/geochemj.1.0105

Ko R, Smith LT, Smith GM (1994) Glycine betaine confers enhanced osmotolerance and cryotolerance on *Listeria monocytogenes*. J Bacteriol 176:426–431

Kouril T, Zaparty M, Marrero J, Brinkmann H, Siebers B (2008) A novel trehalose synthesizing pathway in the hyperthermophilic Crenarchaeon *Thermoproteus tenas*: the unidirectional TreT pathway. Arch Microbiol 190:355–369. doi:10.1007/s00203-008-0377-3

Krulwich TA, Guffanti AA (1989) The $Na^+$ cycle of extreme alkalophiles: a secondary $Na^+/H^+$ antiporter and $Na^+$/solute symporters. J Bioenerg Biomembr 21:663–677. doi:10.1007/BF00762685

Krulwich TA, Sachs G, Padan E (2011) Molecular aspects of bacterial pH sensing and homeostasis. Nat Rev Microbiol 9:330–343. doi:10.1038/nrmicro2549

Lamark T, Styrvold OB, Strøm AR (1992) Efflux of choline and glycine betaine from osmoregulating cells of *Escherichia coli*. FEMS Microbiol Lett 96:149–154

Lee CS, Li XD, Shi WZ, Cheung SC, Thornton I (2006) Metal contamination in urban, suburban, and country park soils of Hong Kong: a study based on GIS and multivariate statistics. Sci Total Environ 356:45–61. doi:10.1016/j.scitotenv.2005.03.024

Levina N, Totemeyer S, Stokes NR, Louis P, Jones MA, Booth I (1999) Protection of *Escherichia coli* cells against extreme turgor by activation of MscS and MscL mechanosensitive channels: identification of genes required for MscS activity. EMBO J 18:1730–1737. doi:10.1093/emboj/18.7.1730

Lopez CS, Alice AF, Heras H, Rivas EA, Sanchez-Rivas C (2006) Role of anionic phospholipids in the adaptation of *Bacillus subtilis* to high salinity. Microbiology 152:605–616. doi:10.1099/mic.0.28345-0

Mana-Capelli S, Mandal AK, Argüello JM (2003) *Archaeoglobus fulgidus* CopB is a thermophilic $Cu^{2+}$-ATPase: functional role of its histidine-rich-N-terminal metal binding domain. J Biol Chem 278:40534–40541. doi:10.1074/jbc.M306907200

McLean RJ, Beauchemin D, Clapham L, Beveridge TJ (1990) Metal-binding characteristics of the gamma-glutamyl capsular polymer of *Bacillus licheniformis* ATCC 9945. Appl Environ Microbiol 56:3671–3677

Nakamura T, Yamamuro N, Stumpe S, Unemoto T, Bakker EP (1998) Cloning of the *trkAH* gene cluster and characterization of the Trk $K^+$-uptake system of *Vibrio alginolyticus*. Microbiology 144:2281–2289. doi:10.1099/00221287-144-8-2281

Nunes-Alves C (2016) Microbial ecology: do it yourself nitrification. Nat Rev Microbiol 14:61–61. doi:10.1038/nrmicro.2015.20

Ohta S, Kim D (2001) Submersible observations at the hydrothermal vent communities on the Iheya Ridge, Mid Okinawa Trough, Japan. J Oceanogra 57:663–677. doi:10.1023/A:1021620023610

Palmgren MG, Nissen P (2011) P-type ATPase. Annu Rev Biophys 40:243–266. doi:10.1146/annurev.biophys.093008.131331

Pikuta EV, Hoover RB, Tang J (2007) Microbial extremophiles at the limits of life. Crit Rev Microbiol 33:183–209. doi:10.1080/10408410701451948

Prieur D, Erauso G, Jeanthon C (1995) Hyperthermophilic life at deep-sea hydrothermal vents. Planet Space Sci 43:115–122. doi:10.1016/0032-0633(94)00143-F

Rensing C, Mitra B, Rosen BP (1997) The *zntA* gene of *Escherichia coli* encodes a Zn(II)-translocating P-type ATPase. Proc Natl Acad Sci USA 94:14326–14331. doi:10.1073/pnas.94.26.14326

Romantsov T, Helbig S, Culham DE, Gill C, Stalker L, Wood JM (2007) Cardiolipin promotes polar localization of osmosensory transporter ProP in *Escherichia coli*. Mol Microbiol 64:1455–1465. doi:10.1111/j.1365-2958.2007.05727.x

Romantsov T, Guan Z, Wood JM (2009) Cardiolipin and the osmotic stress responses of bacteria. Biochim Biophys Acta 1788:2092–2100. doi:10.1016/j.bbamem.2009.06.010

Roosild TP, Miller S, Booth IR, Choe S (2002) A mechanism of regulating transmembrane potassium flux through a ligand-mediated conformational switch. Cell 109:781–791. doi:10.1016/S0092-8674(02)00768-7

Ruff SE, Biddle JF, Teske AP, Knittel K, Boetius A, Ramette A (2015) Global dispersion and local diversification of the methane seep microbiome. Proc Natl Acad Sci USA 112:4015–4020. doi:10.1073/pnas.1421865112

Sakai H, Gamo T, Kim ES, Shitashima K, Yanagisawa F, Tsutsumi M, Ishibashi J, Sano Y, Wakita H, Tanaka T, Matsumoto T, Naganuma T, Mitsuzawa K (1990) Unique chemistry of the hydrothermal solution in the mid-Okinawa Trough backarc basin. Geo Res Lett 17:2133–2136. doi:10.1029/GL017i012p02133

Sans N, Schindler U, Schroder J (1988) Ornithine cyclodeaminase from Ti plasmid C58: DNA sequence, enzyme properties and regulation of activity by arginine. Eur J Biochem 173:123–130. doi:10.1111/j.1432-1033.1988.tb13975.x

Sibuet JC, Letouzey J, Barbier F, Charvet J, Foucher JP, Hilde TW, Kimura M, Chiao LY, Marsset B, Muller C, Stéphan JF (1987) Back arc extension in the Okinawa Trough. J Geophys Res 92:14041–14063

Silver S (1996) Bacterial resistances to toxic metal ions—a review. Gene 179:9–19. doi:10.1016/S0378-1119(96)00323-X

Singer E, Emerson D, Webb EA, Barco RA, Kuenen JG, Nelson WC, Chan CS, Comolli LR, Ferriera S, Johnson J, Heidelberg JF, Edwards KJ (2011) *Mariprofundus ferrooxydans* PV-1 the first genome of a marine Fe(II) oxidizing *Zetaproteobacterium*. PLoS ONE 6:e25386. doi:10.1371/journal.pone.0025386

Sleator RD, Hill C (2001) Bacterial osmoadaptation: the role of osmolytes in bacterial stress and virulence. FEMS Microbiol Rev 26:49–71. doi:10.1016/S0168-6445(01)00071-7

Sleator RD, Gahan CGM, Hill C (2001) Identification and disruption of the *proBA* locus in *Listeria monocytogenes*: role of proline biosynthesis in salt tolerance and murine infection. Appl Environ Microbiol 67:2571–2577. doi:10.1128/AEM.67.6.2571-2577.2001

Slonczewski JL, Fujisawa M, Dopson M, Krulwich TA (2009) Cytoplasmic pH measurement and homeostasis in bacteria and archaea. Adv Microb Physiol 55:1–79. doi:10.1016/S0065-2911(09)05501-5

Speelmans G, Poolman B, Konings WN (1995) $Na^+$ as coupling ion in energy transduction in extremophilic Bacteria and Archaea. World J Microbiol Biotechnol 11:58–70. doi:10.1007/BF00339136

Strøm AR, Falkenberg P, Landfald B (1986) Genetics of osmoregulation in *Escherichia coli*: uptake and biosynthesis of organic osmolytes. FEMS Microbiol Rev 39:79–86. doi:10.1016/0378-1097(86)90064-9

Sukharev SI, Blount P, Martinac B, Blattner FR, Kung C (1994) A large-conductance mechanosensitive channel in *E. coli* encoded by MscL alone. Nature 368:265–268. doi:10.1038/368265a0

Sun QL, Wang MQ, Sun L (2015) Characteristics of the cultivable bacteria from sediments associated with two deep-sea hydrothermal vents in Okinawa Trough. World J Microbiol Biotechnol 31:2025–2037. doi:10.1007/s11274-015-1953-8

Tabor CW, Tabor H (1985) Polyamines in microorganisms. Microbiol Rev 49:81–99

Takaki Y, Shimamura S, Nakagawa S, Fukuhara Y, Horikawa H, Ankai A, Harada T, Hosoyama A, Oguchi S, Fukui S, Fujita N, Takami H, Takai K (2010) Bacterial lifestyle in a deep-sea hydrothermal vent chimney revealed by the genome sequence of the thermophilic bacterium *Deferribacter desulfuricans* SSM1. DNA Res 17:123–137. doi:10.1093/dnares/dsq005

Takami H, Nakasone K, Takaki Y, Maeno G, Sasaki R, Masui N, Fuji F, Hirama C, Nakamura Y, Ogasawara N, Kuhara S, Horikoshi K (2000) Complete genome sequence of the alkaliphilic bacterium *Bacillus halodurans* and genomic sequence comparison with *Bacillus subtilis*. Nucleic Acids Res 28:4317–4331. doi:10.1093/nar/28.21.4317

Takami H, Takaki Y, Uchiyama I (2002) Genome sequence of *Oceanobacillus iheyensis* isolated from the Iheya Ridge and its unexpected adaptive capabilities to extreme environments. Nucleic Acids Res 30:3927–3935. doi:10.1093/nar/gkf526

Takami H, Takaki Y, Chee GJ, Nishi S, Shimamura S, Suzuki H, Matsui S, Uchiyama I (2004) Thermoadaptation trait revealed by the genome sequence of thermophilic *Geobacillus kaustophilus*. Nucleic Acids Res 32:6292–6303. doi:10.1093/nar/gkh970

Tamura K, Stecher G, Peterson D, Filipski A, Kumar S (2013) MEGA6: molecular evolutionary genetics analysis version 6.0. Mol Biol Evol 30:2725–2729. doi:10.1093/molbev/mst197

Thornburg CC, Zabriskie TM, McPhail KL (2010) Deep-sea hydrothermal vents: potential hot spots for natural products discovery? J Nat Prod 73:489–499. doi:10.1021/np900662k

Tokeshi M (2011) Spatial structures of hydrothermal vents and vent-associated megafauna in the back-arc basin system of the Okinawa Trough, western Pacific. J Oceanogr 67:651–665. doi:10.1007/s10872-011-0065-9

Tsuji T, Takai K, Oiwane H, Nakamura Y, Masaki Y, Kumagai H, Kinoshita M, Yamamoto F, Okano T, Kuramoto S (2012) Hydrothermal fluid flow systems around the Iheya North Knoll in the mid-Okinawa trough based on seismic reflection data. J Volcanol Geoth Res 213–214:41–50. doi:10.1016/j.jvolgeores.2011.11.007

Uchida I, Sekizaki T, Hashimoto K, Terakado N (1985) Association of the encapsulation of *Bacillus anthracis* with a 60 megadalton plasmid. J Gen Microbiol 131:363–367

Wang HL, Sun L (2016) Comparative metagenomic analysis of the microbial communities in the surroundings of Iheya north and Iheya ridge hydrothermal fields reveals insights into the survival strategy of microorganisms in deep-sea environments. J Marine Syst. doi:10.1016/j.jmarsys.2016.10.006

Yanagawa K, Nunoura T, McAllister SM, Hirai M, Breuker A, Brandt L, House CH, Moyer CL, Birrien JL, Aoike K, Sunamura M, Urabe T, Mottl MJ, Takai K (2013) The first microbiological contamination assessment by deep-sea drilling and coring by the D/V Chikyu at the Iheya North hydrothermal field in the Mid-Okinawa Trough (IODP Expedition 331). Front Microbiol 4:327. doi:10.3389/fmicb.2013.00327

Yanagawa K, Breuker A, Schippers A, Nishizawa M, Ijiri A, Hirai M, Takaki Y, Sunamura M, Urabe T, Nunoura T, Takai K (2014) Microbial community stratification controlled by the subseafloor fluid flow and geothermal gradient at the Iheya North hydrothermal field in the Mid-Okinawa Trough (Integrated Ocean Drilling Program Expedition 331). Appl Environ Microbiol 80:6126–6135. doi:10.1128/AEM.01741-14

Zhang Y, Rock CO (2008) Membrane lipid homeostasis in bacteria. Nat Rev Microbiol 6:222–233. doi:10.1038/nrmicro1839

Zhang J, Sun QL, Zeng ZG, Chen S, Sun L (2015) Microbial diversity in the deep-sea sediments of Iheya North and Iheya Ridge, Okinawa Trough. Microbiol Res 177:43–52. doi:10.1016/j.micres.2015.05.006